



COMPARATIVE EVALUATION OF THE TOXICOLOGICAL EFFECTS OF GOLD AND SILVER NANOPARTICLES ON THE ALVEOLAR BONE OF ALBINO RATS

Hebatallah Howeidy^{*,**} , Tahany Haggag^{*} ,
Samah Mohamed Kamel^{**}  and Nermeen AbuBakr^{*} 

ABSTRACT

Objectives: Gold and silver nanoparticles (AuNPs and AgNPs) are two of the most commonly used nano materials owing to their remarkable characteristics. However, researchers have not yet compared their toxicological effects on oral tissues. Thus, this study intended to assess and contrast the toxicological impacts of AuNPs and AgNPs on alveolar bone of albino rats.

Methods: Eighteen male albino rats were randomly allocated into three equal groups. Group I: control group, groups II and III (AuNPs and AgNPs groups) received a daily intraperitoneal injection of 4mg/kg of AuNPs or AgNPs, respectively for five weeks. Rats were then euthanized, and the mandibular alveolar bone was studied via histological, histochemical, and histomorphometric analyses and real-time polymerase chain reaction (qRT-PCR) assessment for nuclear factor kappa beta (NF- κ B).

Results: Histological and histochemical results showed normal bone structure in the control group. In the gold group, some signs of degeneration were observed which were more aggravated in the silver group. Histomorphometric analysis of the osteoblastic count and area percentage of mineralized bone confirmed the histological and histochemical results revealing the lowest values in the silver group followed by the gold group then the control group. NF- κ B mRNA expression was significantly elevated in the silver group in comparison to the gold group and relative to the control group.

Conclusion: In conclusion, AgNPs showed more toxic effects than AuNPs, likely due to their production of higher oxidative stresses.

KEY WORDS: Alveolar bone, Gold nanoparticles, Silver nanoparticles, Oxidative stress

* Oral Biology Department, Faculty of Dentistry, Cairo University, Cairo, Egypt

** Oral Biology Department, Faculty of Dentistry, Modern Science and Arts University (MSA), 6th of October, Egypt

INTRODUCTION

Nanotechnology is a multidisciplinary scientific domain that enabled the development of effective dental and medical treatments ^[1,2]. Every field of dentistry is being transformed extensively by nanodentistry. This includes supporting aids for maintaining dental hygiene, as well as therapeutic and diagnostic instruments, the use of drug release cargo in nano dental adducts in prosthodontic, orthodontic, and regeneration treatments ^[3].

Nanoparticles (NPs) can penetrate the body easily without causing cell damage. Among the most widely produced nanoparticles are gold, silver, palladium, selenium, zinc, cobalt, cadmium, aluminum, nickel and iron. The remarkable biocompatible, visual, catalytic, and antibacterial qualities of noble metal nanoparticles make them stand out. Gold and silver NPs usually exhibit superior stability and adjustable surface chemistry than other metals or metal oxide NPs ^[3,4].

Gold nanoparticles (AuNPs) are tiny clusters of gold atoms manufactured from the reduction of gold salts in specific reagents. It is biocompatible, readily bio conjugable, and promising for use in biomedical imaging, diagnostics, and therapeutic applications^[5]. AuNPs are favored owing to their low toxicity, ease of detection, and simplicity in manufacturing and functionalization. Growth factors and DNA are coupled with chitosan-AuNPs on implant surface to promote osseointegration ^[6].

Silver nanoparticles (AgNPs) are a form of metal colloidal NPs prepared by reduction of silver salts in appropriate solutions. They are known for their unique physicochemical properties ^[7]. They are commonly utilized in antimicrobial dressings, medical devices, and cosmetics. In nanodentistry, AgNPs were found to improve oral health and general well-being by decreasing bacterial populations in different dental composites. AgNPs are also incorporated in dental prostheses, implants, and restorative material ^[8].

The in vivo performance and physical stability of nanoparticles can be dictated by both their diameter and surface properties. The size, concentration, and surface functionalization of NPs influence their in vivo bio-distribution and toxicity results ^[9]. It was stated that smaller NPs have more cytotoxicity than larger ones. But regardless of the nanoparticle size, it was shown that dose-dependency, not size, was what caused the cytotoxicity ^[10]. This makes it difficult to thoroughly investigate how the biological system reacts to the administration of NPs, especially given the diversity and variety of human cells and tissues ^[11].

Therefore, the present work sought to inspect and contrast the toxic effects of both AuNPs and AgNPs, having the same size, taken with the same dose and duration on alveolar bone of albino rats via histopathological, histochemical, and histomorphometric methods and via gene expression analysis of nuclear factor kappa beta (NF- κ B).

MATERIALS AND METHODS

Gold and Silver nanoparticles

Gold and silver nanoparticles were acquired from Nano Gate lab. Both nanoparticles were prepared by chemical reduction method ^[12, 13]. To examine the produced nanoparticles, a transmission electron microscope (TEM; JEOL JEM-2100) was utilized at an increasing voltage of 200 kV.

Sample size calculation

Regarding the primary outcome (osteoblasts count at end point 5 weeks), it was found that 5 rats will be appropriate sample size for each group, with an entire sample size of 15 rats. The α error probability =0.05, power =80% and the effect size =0.92. The number increased to 18 rats to compensate for the dropout of 15%. The magnitude of the effect to be identified was approximated as percentage of the variable of interest attained from the previous work by Shawky et al. ^[14]. PS software was used to investigate the sample size.

Animals

In the current study, 18 male adult albino rats (4-6 months age and 200-250 g) were employed. Rats were obtained from Cairo University's Faculty of Medicine's animal house. The rats were preserved in a controlled setting with 12-hour cycles of dark and light and a temperature of $25\pm 2^{\circ}\text{C}$. The rats were given their basic diet of ordinary rat chow and water ad libitum.

Animal grouping

Animals were allocated randomly into 3 groups, 6 rats each as follows:

Group I (Control group): rats were injected daily with saline intraperitoneally for 5 weeks.

Group II (AuNPs group): rats obtained a daily intraperitoneal injection of 4 mg/kg of AuNPs (50nm) for 5 weeks [15, 16].

Group III (AgNPs group): rats obtained a daily intraperitoneal injection of 4 mg/kg of AgNPs (50nm) for 5 weeks [17, 18].

At the end of five-week duration, every rat was euthanized by a mixture of ketamine and xylazine overdose [19]. The mandibles were obtained and subjected to:

Light microscopic examination

The right and left mandibular jaws were separated after being dissected. The right halves were fixed for 24 hours in 10% formaldehyde, then they were decalcified for 28 days at 4°C in 15% EDTA. Following decalcification, jaws were washed with buffer, dehydrated in ethyl alcohol, cleaned in xylol, and then embedded in wax. From

a rotary micrometer, 4-6 μm sagittal sections were taken, positioned on glass slides, and stained using hematoxylin and eosin (H&E) or Masson trichrome stains [20].

Histomorphometric analysis

Leica QWin 500 image processing and analysis software (Leica Microsystems GmbH, Wetzlar, Germany) was used to assess the H&E and Masson trichrome-stained sections to calculate the osteoblast count and to determine the area percent of mineralized bone [21].

Quantitative real-time polymerase chain reaction (qRT-PCR)

A high-capacity cDNA reverse transcriptase kit was utilized to reverse-transcribe 1000 ng of the total RNA from every sample to form cDNA [22]. Then, using a Step One device (Applied Biosystems), cDNA was amplified on a 48-well plate using a Syber Green I PCR Master Kit (Fermentas, Waltham, USA) as follows: The amplification stage involved 40 cycles of 15 seconds at 95°C , 20 seconds at 55°C , and 30 seconds at 72°C following 10 minutes at 95°C to activate the enzyme [23]. Beta actin (β -actin) was used as a housekeeping gene.

Statistical analysis

SPSS version 22 was the statistical software utilized to code and record data. The mean and standard deviation were used to summarize the data. Applying the Kolmogorov-Smirnov test, the data were studied for normality. Analysis of variance (ANOVA) was applied to compare various outcomes for normally distributed data, and the post hoc test was utilized for pairwise comparisons.

TABLE (1). Primer sequence of examined genes.

Gene	Forward	Reverse	Accession number
NF- κ B	5'-CGCGGGGACTATGACTTGAA-3'	5'-AGTTCCGGTTTACTCGGCAG-3'	NM_199267.2
β -actin	5'-CTATGTTGCCCTAGACTTCG-3'	5'-AGGTCTTTACGGATGTCAAC-3'	NM_031144.3

Pearson's correlation was used to perform the correlations. P values below 0.05 were regarded as statistically significant.

RESULTS

TEM examination of the prepared nanoparticles

TEM examination of the prepared AuNPs and AgNPs showed spherical shaped particles. The average particle size appeared to be 50 ± 5 nm (**Fig. 1**).

Histopathological results

In the control group, the alveolar bone appeared with normal interconnected bone trabeculae composed of lamellar bone and enclosing narrow marrow spaces. Haversian and Volkmann's canals were noticed. The trabeculae contained regularly spaced lacunae, each containing an intact osteocyte denoting viable bone tissue. Osteoclasts were noticed at the periphery of periodontal ligaments indicative of normal bone remodeling activity (**Fig. 2a, d**). In the gold group, bone trabeculae were irregular and normal bone architecture was disrupted. However, most lacunae of osteocytes were intact but with few empty lacunae. The bone marrow spaces were of normal size but infiltrated with few inflammatory cells and extravasated red blood cells. The bone marrow lining was devoid of cells. Reversal lines were apparent denoting active bone resorption (**Fig. 2b, e**). In the silver group, the bone trabeculae and overall architecture were more severely disrupted compared to the gold

group. The marrow spaces were increased in size and were highly infiltrated with inflammatory cells. The lining of the marrow cavity was completely devoid of cellular component. Most lacunae of osteocytes were empty denoting degeneration of osteocytes. More numerous reversal lines were observed suggestive of increased bone remodeling and resorptive activity (**Fig. 2c, f**).

Histochemical results

Masson trichrome staining results revealed normal mineralized bone in the control group which appeared as pink colour (**Fig. 3a**). The gold group showed pink staining in approximately all the tissue denoting viable mineralized bone tissue but to a lesser degree than the normal group (**Fig. 3b**). The silver group showed few areas with pink colour while the rest of the tissue appeared blue indicative of unmineralized bone tissue confirming the disturbance of bone mineralization (**Fig. 3c**).

Histomorphometric results

Statistical analysis of the osteoblastic count and the area percentage of mineralized bone revealed a substantial variation among all groups utilizing ANOVA ($p < 0.001$). There was a significant decrease in osteoblastic count and bone area percentage in silver and gold groups in contrast to the control group. Furthermore, a significant decline in osteoblastic count and bone area percentage was reported in the silver group in comparison to the gold group ($p < 0.001$) (**Fig. 3d**).

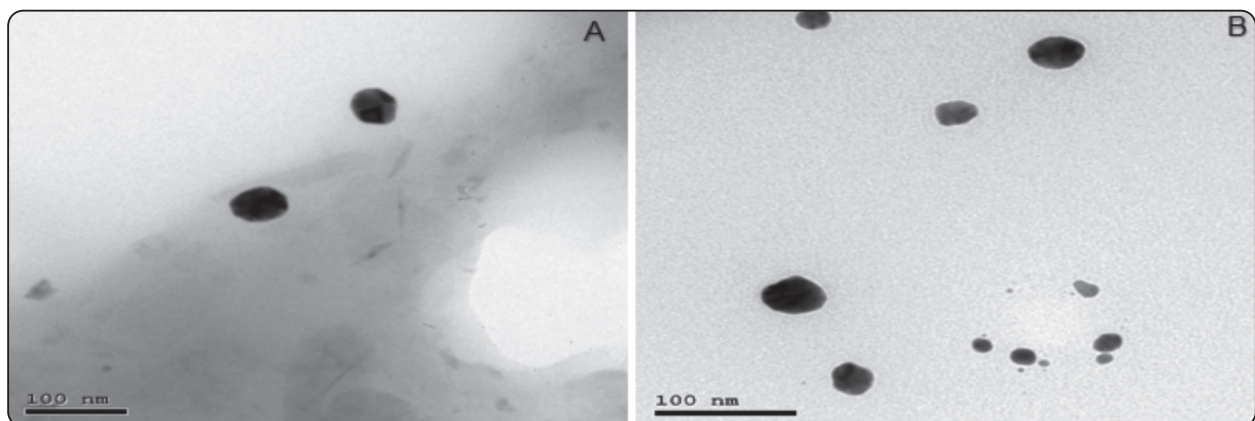


Fig. (1) A photomicrograph showing the TEM images of (a) AuNPs, (b) AgNPs.

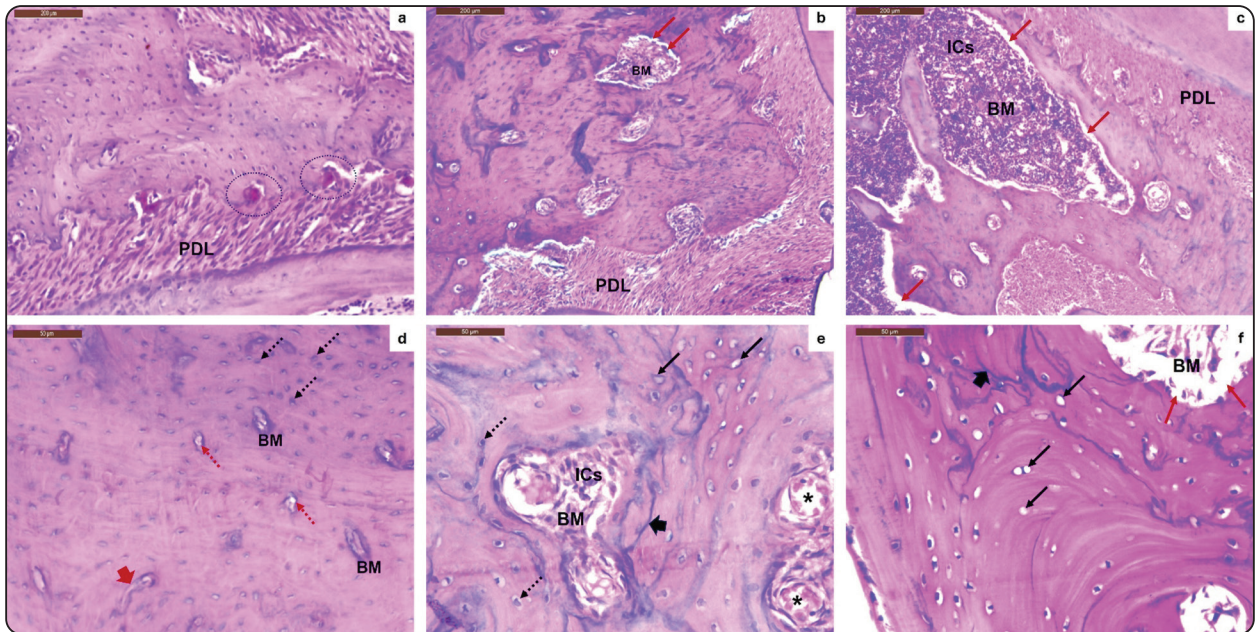


Fig. (2) A photomicrograph showing the alveolar bone of (a, d) Control group, (b, e) AuNPs group, (c, f) AgNPs group revealing periodontal ligaments (PDL), osteoclasts (dotted circles), osteocytes (dotted arrows), haversian canals (dotted red arrows), Volkmann's canal (red arrow head), bone marrow cavities (BM), lining of bone marrow cavity (red arrows), empty lacunae (black arrows), reversal lines (black arrow heads), inflammatory cells infiltrate (ICs), extravasated red blood cells (asterisks) (H&E, Orig. Mag. a-c $\times 100$, d-f $\times 400$).

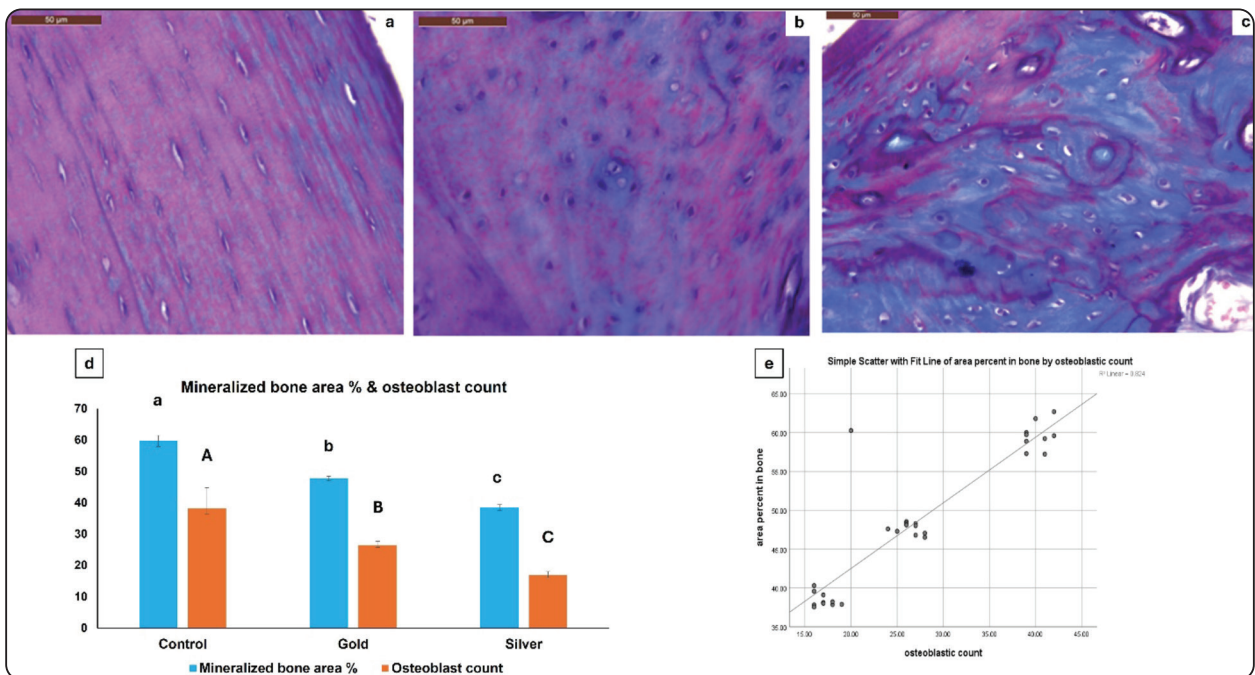


Fig. (3) A photomicrograph showing bone mineralization. (a) Control group, (b) AuNPs group, (c) AgNPs group (Masson Trichrome, Orig. Mag. $\times 400$). (d) A bar chart showing area percentage of mineralized bone and osteoblastic count. Bars with different letters are significantly different. Small letters for area percentage and capital letters for osteoblastic count. (e) Correlation between osteoblastic count and area percentage of mineralized bone.

Correlation between osteoblast count and area percentage of bone

A statistically significant positive association was witnessed between osteoblastic count and area percentage of mineralized bone (P value <0.001, $r=0.908$) (Fig. 3e).

qRT-PCR results

NF- κ B gene expression examination using ANOVA exhibited a significant variation across all groups ($p < 0.001$). There was a significant increase in NF- κ B gene expression in silver and gold groups in contrast to the control group. Furthermore, there was a substantial increase in NF- κ B gene expression in the silver group compared to gold group ($p < 0.001$) (Fig. 4).

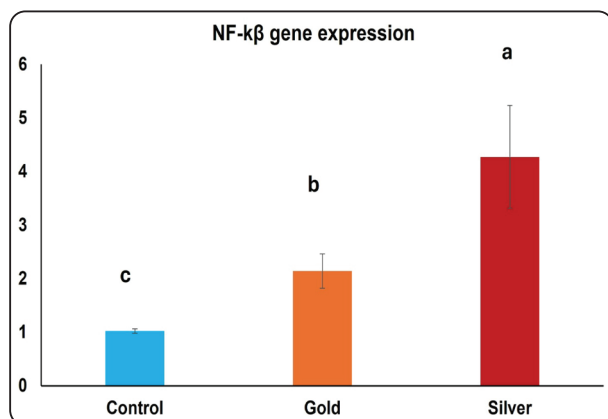


Fig. (4) A bar chart showing NF- κ B gene expression. Bars with different letters are significantly different.

DISCUSSION

The toxicological effects of AuNPs and AgNPs compared to each other on the alveolar bone have not been investigated. Hence, this research intended to investigate and compare the toxicological effects of AuNPs and AgNPs, having the same size, taken with the same dose and duration on the alveolar bone of albino rats via histological, histochemical, histomorphometric, and molecular examination.

In this study, rats were given 4 mg/kg body weight/day of AuNPs [15, 16] or AgNPs [17, 18] intraperitoneally

for five weeks (particle size 50 nm). The choice of particle dose and size was in accordance with previous studies since these parameters are critical determinants of nanoparticle toxicity.

Numerous studies investigating the nanotoxicity of AuNPs and AgNPs have used size range of 10–100 nm in their research. Nanoparticles within this range are small enough to interact effectively with biological systems, yet large enough to avoid rapid renal clearance [24]. Zhang et al. [25] highlighted the influence of nanoparticle dimension on cellular uptake, emphasizing that nanoparticles around 50 nm exhibit optimal endocytosis and accumulations in organs such as spleen and liver. They also documented that smaller nanoparticles (<10 nm) exhibit higher toxicity due to their enhanced competence to penetrate cell membranes and nuclei, while larger nanoparticles (>100 nm) show reduced cellular uptake and lower toxicity.

In the present work, the histological evaluation of the AuNPs group revealed nearly normal histology with mild degenerative signs compared to the control group and, conversely, better histology compared to the AgNPs group, which showed more degenerative histopathological changes. Consistent with our findings, Zhang et al. [25] stated that no morphological alterations were seen after AuNPs administration. However, AuNPs were absorbed by osteoblasts and gathered in vesicular structures and the perinuclear compartment. Moreover, Gao et al. [26] highlighted that AuNPs promoted osteogenic differentiation and inhibited osteoclast formation, making them promising candidates for osteoporosis treatment. The study emphasized that AuNPs exhibited optimal osteogenic effects, aligning with our observations of mild histological impacts of AuNPs on alveolar bone.

On the contrary, Youssef and Saied [27] reported tissue atrophy and NF- κ B activation in rat palatal tissues after administration of AuNPs. Similarly, El-Drieny et al. [28] found neuronal deposition of AuNPs and astrogliosis in rat brains after prolonged

exposure. These findings indicate that the biocompatibility of AuNPs depends on dose and context with higher concentrations or longer exposure times leading to adverse effects.

The degenerative histopathological findings observed in the AgNPs group were consistent with previous work where significant tissue degeneration and inflammation following treatment with AgNPs were observed in the pulp and spleen of albino rats, respectively [29, 30]. The cytotoxic effects of AgNPs are likely mediated through mechanisms such as the release of reactive oxygen species (ROS), silver ions, mitochondrial membrane damage, and the initiation of apoptosis [31]. Hou et al. [32] concluded that AgNPs damaged the breast tissue in clinical applications through increasing cellular oxidative stress, causing mitochondrial alteration.

However, contrary to our findings, Frankova et al. [33] described a noteworthy reduction in number of inflammatory cells upon AgNPs administration, with reduced levels of pro-inflammatory markers such interleukin-12 (IL-12), vascular endothelial growth factor (VEGF) and tumor necrosis factor (TNF).

The histomorphometric analysis of the osteoblastic count supported the histological findings where an elevated count was recorded in the AuNPs group compared to the AgNPs group. This could be attributed to the osteogenic properties of AuNPs where AuNPs were proved to promote osteoblasts proliferation, enhance alkaline phosphatase, and increase calcium content and number of bone nodules in vitro [25]. AuNPs were also shown to significantly promote osteogenic differentiation by upregulating the major osteogenic markers such as osteocalcin and RUNX2, while also enhancing mineralization in mesenchymal stem cells (MSCs) [34].

The significant decrease in osteoblastic count in the AgNPs group aligned with Youssef et al. [29] who reported that AgNPs induced degeneration and inflammation in dental pulp tissues, leading to reduced cellular activity and tissue damage. In

the same line, Ghosh et al. [35] demonstrated that AgNPs promoted oxidative stress and cytotoxicity in bone marrow cells, resulting in apoptosis and reduced cellular proliferation of osteoblasts. This mechanism likely explains the reduced osteoblastic count observed in the AgNPs group.

Masson's trichrome staining was employed to assess the degree of bone mineralization across the experimental groups. The histochemical analysis revealed distinct patterns of bone mineralization, reflecting the differential impact of AuNPs and AgNPs on bone tissue. In AuNPs group, the bone sections displayed less mineralization in contrast to the control group, suggesting a moderate decline in the degree of mineralization. This finding aligned with the known osteogenic properties of AuNPs, which promoted bone formation but may not fully replicate the mineralization levels observed in healthy bone tissue. On the contrary, Zhang et al. [25] conveyed that AuNPs fully restored bone mineralization to levels comparable to healthy controls. The authors reported no significant differences in mineralization between AuNPs-treated and untreated bone tissue.

As for the AgNPs group, it revealed the presence of poorly mineralized bone matrix, suggesting a substantial reduction in bone mineralization. This pattern reflects a significant impairment in the bone mineralization process, likely due to the cytotoxic effects of AgNPs, which disrupt cellular activity and bone development. This was in accordance with Damle et al. [36] who verified that AgNPs interfered with collagen deposition and mineralization, resulting in poorly mineralized bone matrix. Similarly, Akter et al. [37] reported that AgNPs induced cytotoxicity in bone tissue, leading to reduced mineralization and impaired bone formation.

The molecular analysis in the current study exhibited a substantial elevation in NF- κ B gene expression in silver and gold groups in comparison to the control group. Furthermore, there was considerable upregulation in NF- κ B gene expression

in the silver group compared to the gold group. These findings were in line with previous research where AuNPs were found to activate the canonical NF- κ B pathway in a murine B-lymphocyte cell line [38]. Conversely, other studies have reported inhibitory effects of AuNPs on the activity of NF- κ B where AuNPs significantly reduced NF- κ B binding effect in HepG2 cells, an effect attributed to the anti-inflammatory properties of gold [39]. Similarly, AuNPs stimulated NF- κ B activation and oxidative stress in human astrocytes, but without causing cytotoxicity. The study proposed that AuNPs triggered an adaptive response involving redox-sensitive NF- κ B activation, which may promote cell survival under stress conditions [40]. These findings underscore the dual role of AuNPs in either activating or inhibiting NF- κ B, depending on the cellular context and nanoparticle properties.

The increased expression of NF- κ B in the silver group indicated elevated levels of inflammation and oxidative stress. These discoveries remained compatible with Hou et al. [32] who verified that AgNPs induced ROS production in bone cells, leading to oxidative stress and activation of inflammatory pathways. Their study highlighted that AgNPs disrupted mitochondrial function, resulting in increased ROS levels and subsequent cellular damage.

CONCLUSION

The toxicological impacts of AuNPs and AgNPs on alveolar bone are thoroughly compared in this work. While AuNPs demonstrated favorable biocompatibility and osteogenic potential with mild degenerative changes, AgNPs induced significant histological damage, impaired mineralization, and elevated inflammatory responses. These results demonstrate the significance of choosing the right nanoparticles for biomedical applications, with AuNPs showing promise as a better option for treatments pertaining to bone. However, further research is needed to optimize dosing strategies, functionalization approaches, and long-term safety profiles of these nanoparticles.

Author contributions

H.H., T.H., and N.A. contributed to the conception and design of the study. All authors prepared the figures. Material preparation, data collection, and analysis were performed by all authors. The main manuscript text was written by all authors. All authors revised the manuscript and approved the submission.

Funding

This research did not receive any specific grant from funding agencies in the public, commercial, or not-for-profit sectors.

Data availability

All data generated or analyzed during this study are included in this published article.

Declarations

Ethical approval

The ARRIVE guidelines, as well as the suggestions and endorsement of Cairo University's Institutional Animal Care and Use Committee, were followed in the completion of the current research (approval No. CU/III/F/9/22).

Competing interests

The authors have no relevant financial or non-financial interests to disclose.

REFERENCES

1. Ismail E, Mabrouk M, Salem ZA, AbuBakr N, Beherei H. Evaluation of innovative polyvinyl alcohol/alginate/green palladium nanoparticles composite scaffolds: Effect on differentiated human dental pulp stem cells into osteoblasts. *J Mech Behav Biomed Mater*. 2023;140:105700. <https://doi.org/10.1016/j.jmbbm.2023.105700>
2. Farag DB, Yousry C, Al-Mahallawi AM, El-Askary HI, Meselhy MR, AbuBakr N. The efficacy of *Origanum majorana* nanocubosomal systems in ameliorating submandibular salivary gland alterations in streptozotocin-induced diabetic rats. *Drug Deliv*. 2022;29:62–74. <https://doi.org/10.1080/10717544.2021.2018522>

3. Sreenivasalu PKP, Dora CP, Swami R, Jasthi VC, Shi-roorkar PN, Nagaraja S, et al. Nanomaterials in dentistry: current applications and future scope. *Nanomaterials*. 2022;12:1676. <https://doi.org/10.3390/nano12101676>
4. Burlec AF, Corciova A, Boev M, Batir-Marin D, Mircea C, Cioanca O, et al. Current overview of metal nanoparticles' synthesis, characterization, and biomedical applications, with a focus on silver and gold nanoparticles. *Pharmaceutics*. 2023;16:1410. <https://doi.org/10.3390/ph16101410>
5. Boisselier E, Astruc D. Gold nanoparticles in nanomedicine: preparations, imaging, diagnostics, therapies and toxicity. *Chem Soc Rev*. 2009;38:1759–78. <https://doi.org/10.1039/B806051G>
6. Takanche JS, Kim JE, Kim JS, Lee MH, Jeon JG, Park IS, et al. Chitosan-gold nanoparticles mediated gene delivery of c-myc facilitates osseointegration of dental implants in ovariectomized rat. *Artif Cells Nanomed Biotechnol*. 2018;46:807–17. <https://doi.org/10.1080/21691401.2018.1513940>
7. Dhaka A, Mali SC, Sharma S, Trivedi R. A review on biological synthesis of silver nanoparticles and their potential applications. *Results Chem*. 2023;6:101108. <https://doi.org/10.1016/j.rechem.2023.101108>
8. Fernandez CC, Sokolonski AR, Fonseca MS, Stanisic D, Araújo DB, Azevedo V, et al. Applications of silver nanoparticles in dentistry: advances and technological innovation. *Int J Mol Sci*. 2021;22:2485. <https://doi.org/10.3390/ijms22052485>
9. Hoshyar N, Gray S, Han H, Bao G. The effect of nanoparticle size on in vivo pharmacokinetics and cellular interaction. *Nanomedicine*. 2016;11:673–92. <https://doi.org/10.2217/nnm.16.5>
10. Yang L, Kuang H, Zhang W, Aguilar ZP, Wei H, Xu H. Comparisons of the biodistribution and toxicological examinations after repeated intravenous administration of silver and gold nanoparticles in mice. *Sci Rep*. 2017;7:3303. <https://doi.org/10.1038/s41598-017-03015-1>
11. Mu Q, Jiang G, Chen L, Zhou H, Fourches D, Tropsha A, et al. Chemical basis of interactions between engineered nanoparticles and biological systems. *Chem Rev*. 2014;114:7740–81. <https://doi.org/10.1021/cr400295a>
12. Bastús NG, Comenge J, Puentes V. Kinetically controlled seeded growth synthesis of citrate-stabilized gold nanoparticles of up to 200 nm: size focusing versus Ostwald ripening. *Langmuir*. 2011;27:11098–11105. <https://doi.org/10.1021/la201938u>
13. Turkevich J, Stevenson PC, Hillier J. A study of the nucleation and growth processes in the synthesis of colloidal gold. *Faraday Discuss*. 1951;11:55–75.
14. Shawky HA, Essawy MM. Effect of atorvastatin and remifemine on glucocorticoid induced osteoporosis in rats with experimental periodontitis. *Egypt Dent J*. 2018;64:2287–96. <https://doi.org/10.21608/EDJ.2018.76800>
15. Hassan ZA, Obaid HH, Al-Darraj MN. The toxicity of gold nanoparticles on liver function of albino mice. *Int J Adv Sci Technol*. 2020;29:542–8.
16. Ibrahim KE, Al-Mutary MG, Bakhiet AO, Khan HA. Histopathology of the liver, kidney, and spleen of mice exposed to gold nanoparticles. *Molecules*. 2018;23:1848. <https://doi.org/10.3390/molecules23081848>
17. Elkhawass EA, Mohallal ME, Soliman MF. Acute toxicity of different sizes of silver nanoparticles intraperitoneally injected in Balb/C mice using two toxicological methods. *Int J Pharma Sci*. 2015;7:94–99.
18. El Mahdy MM, Eldin TAS, Aly HS, Mohammed FF, Shaalan MI. Evaluation of hepatotoxic and genotoxic potential of silver nanoparticles in albino rats. *Exp Toxicol Pathol*. 2015;67:21–9. <https://doi.org/10.1016/j.etp.2014.09.005>
19. Soliman T, Ali Z, Zayed M, Sabry D, AbuBakr N. Assessing the bone-healing potential of bone marrow mesenchymal stem cells in jawbone osteoporosis in albino rats. *Dent Med Probl*. 2022;59:75–83. <https://doi.org/10.17219/dmp/139200>
20. AbuBakr N, Fares AE, Mostafa A, Farag DB. Mesenchymal stem cells-derived microvesicles versus platelet-rich plasma in the treatment of monoiodoacetate-induced temporomandibular joint osteoarthritis in Albino rats. *Heliyon*. 2022; 8:e10857. <https://doi.org/10.1016/j.heliyon.2022.e10857>
21. Mohamed HSE, Hegazy RH, Bashir MH, Aboushady IM, Meselhy MR, El-Askary HI, et al. Potential protective role of parsley on induced tongue carcinogenesis in albino rats. *Dent Med Probl*. 2025;62:79–87. <https://doi.org/10.17219/dmp/161507>
22. Mabrouk M, Ismail E, Beherei H, Abo-Elfadl MT, Salem ZA, Das DB, et al. Biocompatibility of hydroxyethyl cellulose/glycine/RuO₂ composite scaffolds for neural-like cells. *Int J Biol Macromol*. 2022;209:2097–2108. <https://doi.org/10.1016/j.ijbiomac.2022.04.190>
23. Abubakr N, Salem Z, Ali Z, Assaly ME. Comparative evaluation of the early effects of the low-level laser therapy versus intra-articular steroids on temporomandibular joint acute osteoarthritis in rats. *Dent Med Probl*. 2018;55:359–66. <https://doi.org/10.17219/dmp/96290>
24. Báez DF, Gallardo-Toledo E, Oyarzún MP, Araya E, Kogan MJ. The influence of size and chemical composition of silver and gold nanoparticles on in vivo toxicity with potential applications to central nervous system diseases.

- Int J Nanomedicine. 2021;16:2187–2201. <https://doi.org/10.2147/IJN.S260375>
25. Zhang D, Liu D, Zhang J, Fong C, Yang M. Gold nanoparticles stimulate differentiation and mineralization of primary osteoblasts through the ERK/MAPK signaling pathway. *Mater Sci Eng C*. 2014;42:70–7. <https://doi.org/10.1016/j.msec.2014.04.042>
 26. Gao W, Liang C, Zhao K, Hou M, Wen Y. Multifunctional gold nanoparticles for osteoporosis: synthesis, mechanism and therapeutic applications. *J Transl Med*. 2023;21:889. <https://doi.org/10.1186/s12967-023-04594-6>
 27. Youssef MM, Saied GM. Histological and immuno-histochemical study of the cytotoxic effects of gold nanoparticles on the palate of albino rats. *Egypt Dent J*. 2019;65:3445–56. <https://doi.org/10.21608/edj.2019.74794>
 28. El-Drieny EAEA, Sarhan NI, Bayomy NA, Elsherbeni SAE, Momtaz R, Mohamed HED. Histological and immunohistochemical study of the effect of gold nanoparticles on the brain of adult male albino rat. *J Microsc Ultrastruct*. 2015;3:181–90. <https://doi.org/10.1016/j.jmau.2015.05.001>
 29. Youssef MM, El-Mansy MN, El-Borady OM, Hegazy EM. Impact of biosynthesized silver nanoparticles cytotoxicity on dental pulp of albino rats. *J Oral Biol Craniofac Res*. 2021;11:386–92.
 30. Mazen NF, Saleh EZ, Mahmoud AA, Shaalan AA. Histological and immunohistochemical study on the potential toxicity of silver nanoparticles on the spleen in adult male albino rats. *Egypt J Histol*. 2017;40:374–87. <https://doi.org/10.21608/EJH.2017.4662>
 31. Wang F, Chen Z, Wang Y, Ma C, Bi L, Song M, et al. Silver nanoparticles induce apoptosis in HepG2 cells through particle-specific effects on mitochondria. *Environ Sci Technol*. 2022;56:5706–13. <https://doi.org/10.1021/acs.est.1c08246>
 32. Hou J, Zhao L, Tang H, He X, Ye G, Shi F, et al. Silver nanoparticles induced oxidative stress and mitochondrial injuries mediated autophagy in HC11 cells through Akt/AMPK/mTOR pathway. *Biol Trace Elem Res*. 2021;199:1062–73. <https://doi.org/10.1007/s12011-020-02212-w>
 33. Franková J, Pivodová V, Vágnerová H, Juráňová J, Ulrichová J. Effects of silver nanoparticles on primary cell cultures of fibroblasts and keratinocytes in a wound-healing model. *J Appl Biomater Funct Mater*. 2016;14:137–42. <https://doi.org/10.5301/jabfm.5000268>
 34. Yi C, Liu D, Fong CC, Zhang J, Yang M. Gold nanoparticles promote osteogenic differentiation of mesenchymal stem cells through p38 MAPK pathway. *ACS Nano*. 2010;4:6439–48. <https://doi.org/10.1021/nn101373r>
 35. Ghosh M, Manivannan J, Sinha S, Chakraborty A, Mallick SK, Bandyopadhyay M, et al. In vitro and in vivo genotoxicity of silver nanoparticles. *Mutat Res Genet Toxicol Environ Mutagen*. 2012;749:60–69. <https://doi.org/10.1016/j.mrgentox.2012.08.007>
 36. Damle A, Sundaresan R, Rajwade JM, Srivastava P, Naik A. A concise review on implications of silver nanoparticles in bone tissue engineering. *Biomater Adv*. 2022;141:213099. <https://doi.org/10.1016/j.bioadv.2022.213099>
 37. Akter M, Sikder MT, Rahman MM, Ullah AA, Hossain KFB, Banik S, et al. A systematic review on silver nanoparticles-induced cytotoxicity: physicochemical properties and perspectives. *J Adv Res*. 2018;9:1–16. <https://doi.org/10.1016/j.jare.2017.10.008>
 38. Sharma M, Salisbury RL, Maurer EI, Hussain SM, Sulentice CE. Gold nanoparticles induce transcriptional activity of NF- κ B in a B-lymphocyte cell line. *Nanoscale*. 2013;5:3747–56. <https://doi.org/10.1039/C3NR30071D>
 39. Kapka-Skrzypczak L, Męczyńska-Wielgosz S, Matysiak-Kucharek M, Czajka M, Sawicki K, Kruszewski M, et al. Nuclear factor kappa B activation by Ag, Au nanoparticles, CdTe quantum dots or their binary mixtures in HepG2 cells. *Ann Agric Environ Med*. 2020;27:231–4. <https://doi.org/10.26444/aaem/120664>
 40. Mytych J, Lewinska A, Zebrowski J, Wnuk M. Gold nanoparticles promote oxidant-mediated activation of NF- κ B and 53BP1 recruitment-based adaptive response in human astrocytes. *Biomed Res Int*. 2015;2015:304575. <https://doi.org/10.1155/2015/304575>